

Optimized Sampling Patterns for Practical Compressed MRI

Muhammad Usman⁽¹⁾ and Philip G. Batchelor⁽¹⁾

(1) Division of Imaging Sciences, Kings College London, United Kingdom
 muhammad.3.usman@kcl.ac.uk, philip.batchelor@kcl.ac.uk

Abstract:

The performance of compressed sensing (CS) algorithms is dependent on the sparsity level of the underlying signal, the type of sampling pattern used and the reconstruction method applied. The higher the incoherence of the sampling pattern used for under-sampling, less aliasing will be noticeable in the aliased signal space, resulting in better CS reconstruction. In this work, based on point spread function (PSF) properties, we compare random, Poisson disc and constrained random sampling patterns and show their usefulness in practical compressed sensing applied to dynamic cardiac magnetic resonance imaging (MRI).

Introduction

One of the main questions that arise in compressed sensing magnetic resonance imaging (CS-MRI) is: which type of sampling is optimal? The basic theory of compressed sensing as proposed by Donoho [1] and Candes [2] requires acquisition of randomized set of measurements. For MRI, this corresponds to the random sampling in Fourier domain (k-space) which results in incoherent aliasing artefacts in image space. However, random sampling requires bigger changes in amplitudes and polarity of MR system gradients, making it infeasible practically in an MR system.

Figure 1 shows one dimensional gradient variations for 2D random and uniform lattice sampling patterns. From the figure, it is evident that we have bigger changes in amplitude and polarity of gradients in case of random sampling pattern than uniform lattice. The solution to this problem is to use deterministic sampling patterns. The uniform lattice pattern is a deterministic pattern but yields coherent artefacts in its PSF and hence, it does not satisfy the basic requirements of compressed sensing theory. Our goal is to find deterministic sampling patterns that have incoherent artefacts in the PSF and can yield better CS reconstruction.

1. Candidate Sampling Patterns in CS

To have minimum aliasing due to sampling below the Nyquist rate, Nayak [3] defined the following properties

of PSF of the ideal sampling pattern: The near zero region around the main lobe of the PSF should be as large as possible and outside that region, PSF should resemble white noise. The samples should be placed randomly but with a restricted maximum distance between samples. These two conditions are met by Poisson disc sampling [4]. Recently, Poisson disc sampling has been shown to give good results in parallel MRI due to better reconstruction conditioning [5]. However, it also has impractical gradient requirements. Gamper [6] defined constrained random pattern with incoherent artefacts in its PSF. Constrained random pattern is a normal lattice pattern with samples shifted along one dimension randomly by -1, 0 and +1. Hence, it is a normal lattice with constrained randomization added along one direction and has moderate gradient requirements. Figure 2 shows the three candidate sampling patterns (random, Poisson disc and constrained random) with the corresponding PSFs. Like Poisson disc sampling, the constrained random sampling has a near-zero region around the main lobe in its PSF and it also possesses the uniform density of sampling both locally and globally.

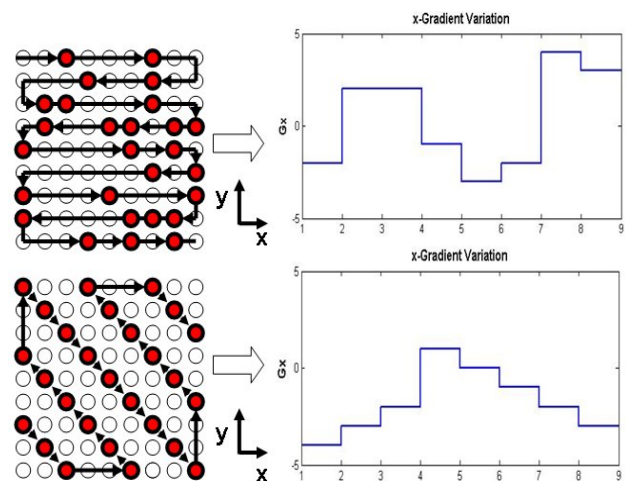


Figure 1: Gradient variation along one dimension in MR system for (a) random sampling (top) (b) uniform lattice sampling (bottom)

Additionally, due to added constrained randomization, the amplitudes of coherent side lobes in the PSF of constrained random pattern are also suppressed. In CS

recovery algorithms like OMP [6] which are based on picking the most significant component from the aliased space iteratively, the suppression of coherent artefacts ensures that only the right candidates are picked up in successive iterations.

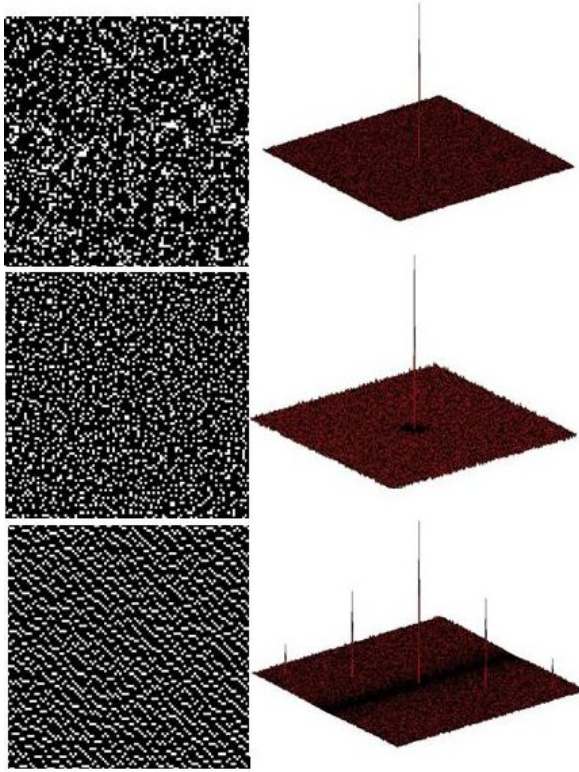


Figure 2: Three candidate sampling patterns and their corresponding PSFs: top to bottom: random, Poisson disc and constrained random

2. Experimental Setup

To test the performance of three sampling patterns in dynamic cardiac MRI, two sets of dynamic cardiac data of size $(n_f \times n_p \times n_x \times n_t, n_f: \text{number of frequency encoding indices}, n_p: \text{number of phase encoding indices}, n_x: \text{number of time frames})$ (224x155x50) and (336x178x48) were acquired with a Philips MRI scanner 1.5 T, SSFP sequence, FOV 350x350 mm². We used the jittered grid approximation of the Poisson disc sampling as proposed by Cook [7]. For CS based reconstruction, the x-f space (x: spatial location, f: temporal frequency) is chosen to be the sparse representation [8]. The x-f space representation of the dynamic cardiac data is obtained by taking the Fourier transform of dynamic MR data along the temporal dimension. Figure 3 shows the dynamic cardiac MR data and its sparse representation.

For each frequency encoding index, the under-sampled data was simulated by applying the three sampling patterns to the fully sampled dynamic cardiac data in k_x -t space (k_x : phase encoding index, t: time) with varying

acceleration factors/sampling factors (SF) from 3 to 7. The x-f space corresponding to each frequency encoding index was independently reconstructed by our modified OMP method with adaptive thresholding scheme [9]. The OMP algorithm stops when maximum residual aliasing intensity in x-f space reaches the intensity level of noise.

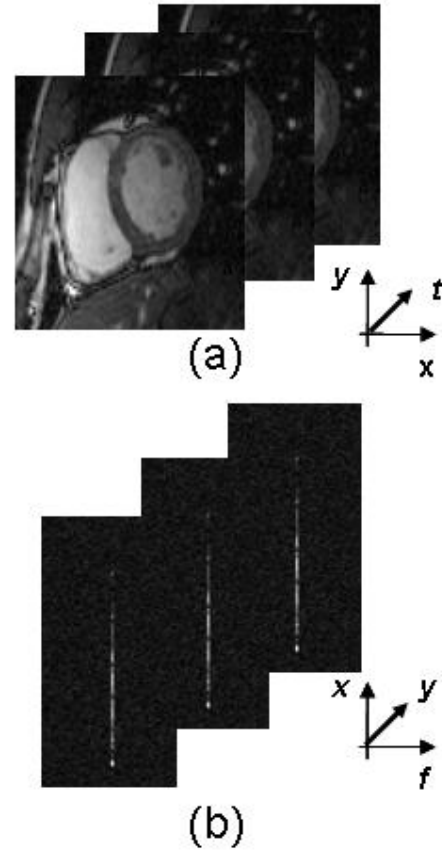


Figure 3: Dynamic cardiac MR data (a) and its x-f space representation (b), the frequency axis 'f' is centered around dc frequency (f=0)

3. Performance Results

The CS reconstruction results for candidate sampling patterns are shown in Figure 4 to Figure 9 with different acceleration factors. For the original cardiac frame shown in Figure 4 (a), the CS reconstruction results by OMP method with under-sampling factor (SF) of 3 are shown in Figure 4 (b), (c) and (d) for random, Poisson disc and constrained random sampling patterns. The corresponding temporal profiles are shown in Figure 5. The CS reconstruction results for acceleration factors of 5 and 7 are shown in Figure 6 to Figure 9. Up to the acceleration factor of 5, the CS reconstructed data has same spatial and temporal resolution for all three sampling patterns with nearly exact signal reconstruction achieved up to SF=3 (Figure 4 and Figure 5). Below SF=5, the temporal resolution of CS reconstructed data

with constrained random sampling gets worse than that for the other sampling patterns (Figure 9 d). This is due to the fact that with very high acceleration factors, many locations within the constrained random pattern will have zero probability of being picked up, as the sampling locations are constrained to only one sample shift from the uniform lattice grid.

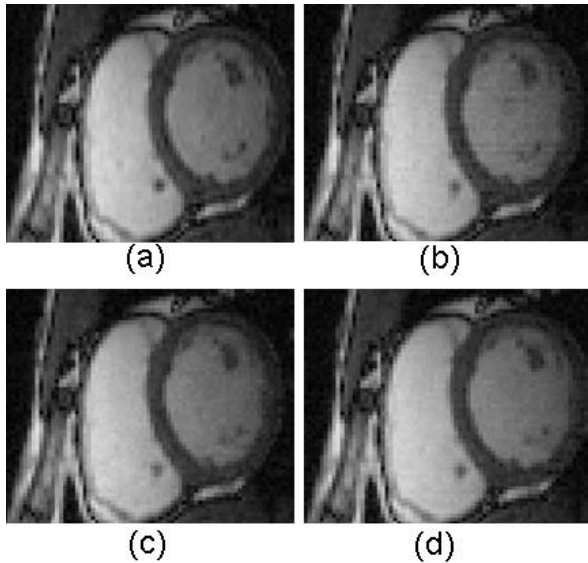


Figure 4: CS reconstruction results with SF=3: (a) original cardiac frame, CS reconstructed data with (b) random sampling (c) Poisson disc sampling (d) constrained random sampling

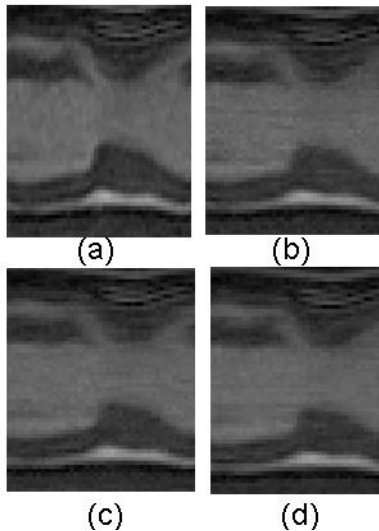


Figure 5: CS reconstruction results with SF=3: (a) original temporal profile, CS Reconstructed temporal profile with (b) random sampling (c) Poisson disc sampling (d) constrained random sampling

pattern (Poisson disc sampling). Up to the acceleration factor of 5, the quality of the reconstructed images and the temporal resolution of the CS reconstructed data are nearly the same for random, Poisson and constrained random sampling patterns. Since the constrained random sampling has moderate gradient requirements when compared with other optimal sampling schemes, it is an excellent choice to be used as an optimal sampling pattern in practical compressed MRI.

References:

- [1] D.L. Donoho, "Compressed Sensing," IEEE transactions on information theory, vol.52, no. 4, pp. 1289-1306, 2006.
- [2] E. Candes, "Compressive sampling," in Proceedings of the International Congress of Mathematicians, vol. 3, pp. 1433-1452, Madrid, Spain, 2006
- [3] KS Nayak et al, "Randomized trajectories for reduced aliasing artifact", in: Proceedings of the ISMRM, p 670., Sydney, 1998
- [4] J. I. Yellot, "Spectral consequences of photoreceptor sampling in the rhesus retina." Science 221, 382-385, 1985
- [5] M. Lustig et al., "Autocalibrating Parallel Imaging Compressed Sensing using L1 SPIR-iT with Poisson-Disc Sampling and Joint Sparsity Constraints ISMRM Workshop on Data Sampling and Image Reconstruction, Sedona '09
- [6] U. Gamper et al, "Compressed sensing in dynamic MRI," MRM, vol. 59, no. 2, pp. 365-373, 2008.
- [7] R. L. Cook, "Stochastic sampling in computer graphics", ACM Transactions on Graphics (TOG), vol.5, no. 1, p. 51-72, Jan 1986
- [8] S. J. Malik et al, "x-f Choice: reconstruction of undersampled dynamic MRI by data-driven alias rejection applied to contrast-enhanced angiography. Stochastic sampling in computer graphics", MRM, vol.56, p. 811-823, 2006
- [9] M. Usman et al, "Adaptive thresholding scheme for OMP method applied to dynamic MRI", Proc. ESMRMB, Valencia, vol. 25, no. 766, pp. 389, Oct 2008

4. Conclusion

We showed that the PSF properties of constrained random sampling are similar to the optimal sampling

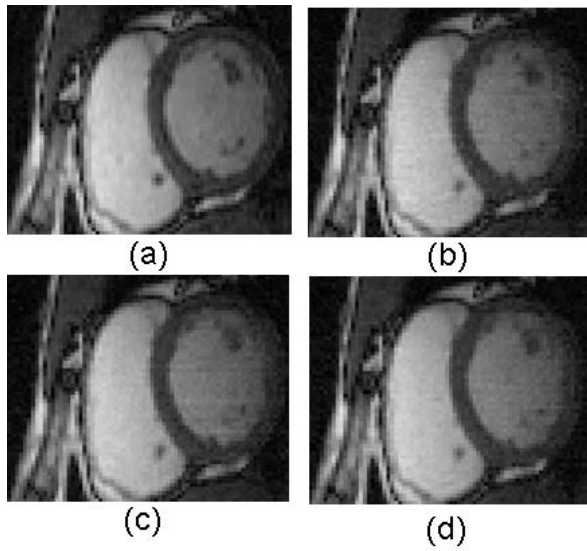


Figure 6: CS reconstruction results with SF=5:
 (a) original cardiac frame, CS reconstructed data with (b) random sampling (c) Poisson disc sampling (d) constrained random sampling

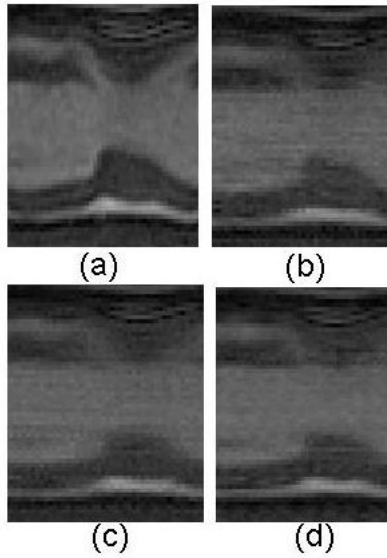


Figure 7:
 CS reconstruction results with SF=5:
 (a)original temporal profile, CS Reconstructed temporal profile with (b) random sampling (c) Poisson disc sampling (d) constrained random sampling

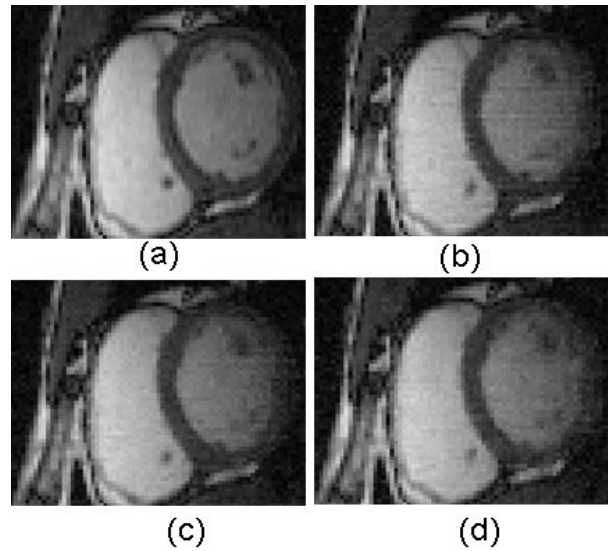


Figure 8: CS reconstruction results with SF=7:
 (a) original cardiac frame, CS reconstructed data with (b) random sampling (c) Poisson disc sampling (d) constrained random sampling

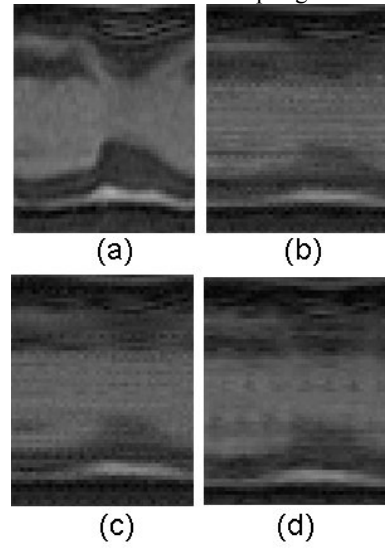


Figure 9:
 CS reconstruction results with SF=7:
 (a)original temporal profile, CS Reconstructed temporal profile with (b) random sampling (c) Poisson disc sampling (d) constrained random sampling